Gun-Launched Satellites

Harold E. Gilreath, Andrew S. Driesman, William M. Kroshl, Michael E. White, Harry E. Cartland, and John W. Hunter

This article summarizes and updates a study conducted for the Defense Advanced Research Projects Agency concerning the technical and economic feasibility of using a distributed-injection, light-gas gun to launch small satellites. In principle, a distributed-injection launcher can produce high muzzle velocities at relatively low acceleration levels. The technical feasibility of such a launcher depends on the successful development of fast injector valves and high-temperature, high-pressure hydrogen heat exchangers. Thermal protection, aerodynamic stability, and packaging are significant, but not insurmountable, challenges in designing a launch vehicle that can withstand high-acceleration loads and survive hypersonic flight across the atmosphere. Although many spacecraft components are readily adapted to high *g* loads, the mass budget of a gun-launched spacecraft is affected substantially by large mass fraction allocations for structure and power subsystems. The results of a financial analysis suggest that a low-volume launch business might provide an attractive total mission cost relative to current systems. (Keywords: Light-gas gun, Small satellites, Space access.)

INTRODUCTION

Just a few years ago, space was the exclusive province of large national governments. Today, more than half of international launches consist of commercial payloads. This rapidly developing space business promises to be very competitive, especially in the telecommunications sector, where more than 20 concepts for low-Earth orbit (LEO) satellite constellations are being pursued. The 66-satellite Iridium constellation is already providing "cell phone in the sky" service worldwide. If all the other concepts being proposed were actually implemented, almost 2800 satellites would be launched between now and the year 2005, not including replacements for failed spacecraft. All of this activity and planning is increasing the pressure to make space access simpler and less costly. Several research and development programs have emerged to develop more economical rockets, mainly by emphasizing reusability. However, orders-of-magnitude reductions in cost will be difficult to achieve.

In September 1997, under the sponsorship of the Defense Advanced Research Projects Agency (DARPA), APL began an assessment of the economic and

technical feasibility of launching payloads in the 10- to 1000-kg range using a gun. In principle, a gun is an attractive alternative to a rocket because it is simple and reusable, and can provide an order-of-magnitude increase in payload fraction. But its disadvantages are substantial, too. The launch vehicle must survive high *g* loads, as well as the severe heating associated with transatmospheric flight at hypersonic speed. Moreover, if the gun is large and immobile, the orbits that can be reached may be limited to a single inclination. If these disadvantages can be mitigated, however, a gun launcher would reflect the "smaller, cheaper" trend in spacecraft design and would offer major improvements in operability, including the ability to launch in all kinds of weather.

Our initial assessment was reported in Ref. 1. In this article, we will discuss the major results from that report and give a brief description of our current work.

BACKGROUND

The first serious efforts in this area were made in the early 1960s under the High Altitude Research Project (HARP),[2] using modified powder guns (Fig. 1). During testing on the island of Barbados and at the Yuma Proving Grounds, gun-launched rockets probed the upper atmosphere to altitudes greater than 100 km. HARP scientists and engineers later developed the techniques and hardware for an orbital vehicle designed to be fired from an extended 16-in. naval gun. They also designed a launcher with an 81-cm bore that could place a 550-kg payload into a 700-km orbit.[3] The sound speed limitation due to the high molecular weight of powder combustion products, together with the relatively short barrel length, meant that the muzzle velocities attainable with HARP launchers were less than 2 km/s. At that level, the launch vehicles had to incorporate multistage rockets to reach the 7+ km/s needed to achieve orbit. The project was terminated before payloads were successfully orbited; however, this early work demonstrated that sensors, electronics, and rockets could survive the rigors of gun launch at accelerations greater than 10,000 *g*.

Figure 1. Firing of the 16-in. HARP gun in Barbados. In the late 1960s and early 1970s, the gun was used to launch rockets as well as scramjets at muzzle velocities up to 1.6 km/s.

In the early 1990s, the Strategic Defense Initiative Office considered a two-stage light-gas gun launcher for deploying the Brilliant Pebbles spacecraft. The requirement was to place up to 4000 spacecraft weighing 100 kg into specified orbits at a rate of one launch every 30 min. Researchers at the Lawrence Livermore National Laboratory analyzed a three-tube, large-scale version of the Super High Altitude Research Project (SHARP) light-gas gun that had been developed earlier by John W. Hunter. They judged the system to be technically feasible.[4]

Using the experience gained in the SHARP project, Harry E. Cartland joined with Hunter in developing detailed conceptual designs for a proposed family of commercial gun launchers, known as the Jules Verne Launcher (JVL) series. These designs were based on the distributed-injection launcher concept, and they provided important information for our study.

The distributed-injection concept is a variation of the light-gas gun design. The launch package is accelerated by injecting working fluid at multiple points along the launch tube rather than having it expand over the entire length from a high-pressure reservoir located at the breech. The concept has been explored previously, both theoretically[5,6] and experimentally,[7] although the experiments were conducted at a scale much smaller than we are considering here. In its application to space launch, the distributed-injection technique is used to reduce the stresses on the launch vehicle (by flattening the acceleration profile) and to facilitate momentum management, rather than to achieve previously unattainable muzzle velocities. In fact, reaching orbit with a single-stage vehicle requires a muzzle velocity in the range of 40 to 50% of the theoretical maximum, which is similar to the documented performance of light-gas guns.[8]

OBJECTIVES AND APPROACH

Affordability was the central focus of this light-gas gun launcher analysis. We were asked to consider practical limitations on the size of the launcher, to define recurring and nonrecurring costs and achievable launch rates, and to compare the economics of gun launchers to that of existing launch systems. We were also asked to identify launch-survivable spacecraft in the 10- to 1000-kg range that might be the basis for a viable

commercial application. The general purpose was to help the government make informed decisions about the development of an operational launch capability based on light-gas gun technology.

The approach we adopted is illustrated in Fig. 2. The initial sizing of the system was based on preliminary construction cost estimates, rough estimates of potential market size, and judgments about technical risk. Because the relative ablation recession length increases rapidly as the size of the launch vehicle decreases, we decided that a system capable of launching spacecraft weighing only tens of kilograms was too risky. However, with construction costs estimated to be over $2 billion, a system capable of launching a 1000-kg spacecraft was considered too expensive, especially for a prototype system. Hence, we focused the study on guns designed to launch 100-kg spacecraft.

To set system requirements, we selected a telecommunications mission similar to the one pursued by "Big LEO" constellations such as Iridium. Our purpose was not to promote a new way to perform global communications, but rather to use the Iridium constellation to uncover the issues associated with launching a complex satellite with a gun. When the effects of the launch environment on spacecraft subsystems were understood, the results could be generalized to other applications. First, we developed a crude set of specifications, shown in Table 1, which assumed that the mission can be completed with a constellation having roughly the same total mass as the Iridium constellation.

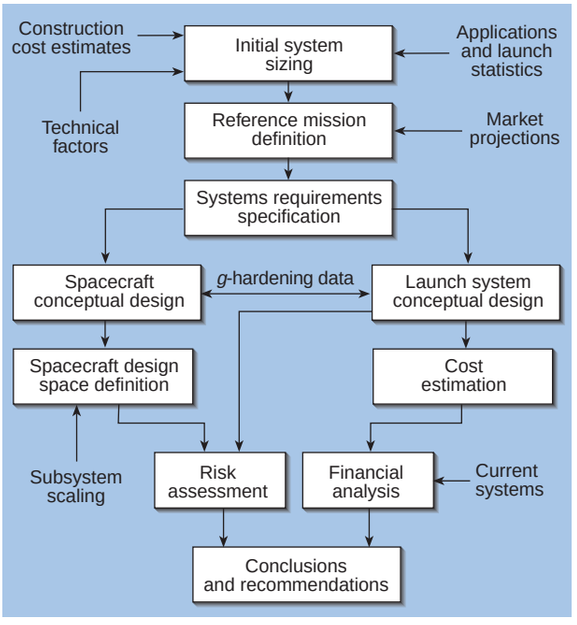

Figure 2. Overall approach to launcher design.

Table 1. Basic system specifications.

System element	Requirement
Orbit altitude	700 km
Orbit inclination	90°
Maximum deployment rate	300/year
Maximum launch rate	2/day
Mission life	5 years
LEO constellation	512 in 32 planes
On-orbit spares	32
Spacecraft mass (wet)	113 kg
Spacecraft volume	0.17 m^3
Spacecraft density	665 kg/m^3
Average axial acceleration	1640 *g*
Peak axial acceleration	2500 *g*
Average lateral acceleration	15 *g*
Vibration loads	1700 *g* @ 25–250 Hz
Launch thermal environment	<320 K

Note: LEO = low-Earth orbit.

LAUNCH SYSTEM

Launcher

The basic requirement set by the mission described in Table 1 is to place a 113-kg spacecraft into a 700-km polar orbit. Vehicle design considerations, discussed below, and ballistic/orbital mechanics resulted in a distributed-injection system capable of launching a 682-kg package at an initial elevation of 22° with a muzzle velocity of 7 km/s. Somewhat arbitrarily, we limited the maximum acceleration to 2500 *g*. This load can be sustained easily by modern electronics with little or no hardening, and is low enough to make survivable designs for more *g*-sensitive components. For practical reasons, gas temperature was limited to 1500 K and peak pressure to 70 MPa, with a target average launch tube pressure of 35 MPa.

With these restrictions, the conceptual launcher has a bore diameter of 63.5 cm and a length of 1.52 km (Fig. 3). The distributed-injection system consists of a base injector and 15 side injector pairs that are separated by 150 launch tube diameters. Each injector comprises a high-pressure hydrogen reservoir, a heat exchanger, and a high-speed valve. A pumping system requires 1 h to charge the high-pressure reservoirs to 70 MPa with hydrogen from a 14-MPa storage reservoir. The high-pressure hydrogen passes through a heat exchanger, reaching 1500 K, before entering the launch tube at an angle of 20° by way of a high-speed valve. Simulations

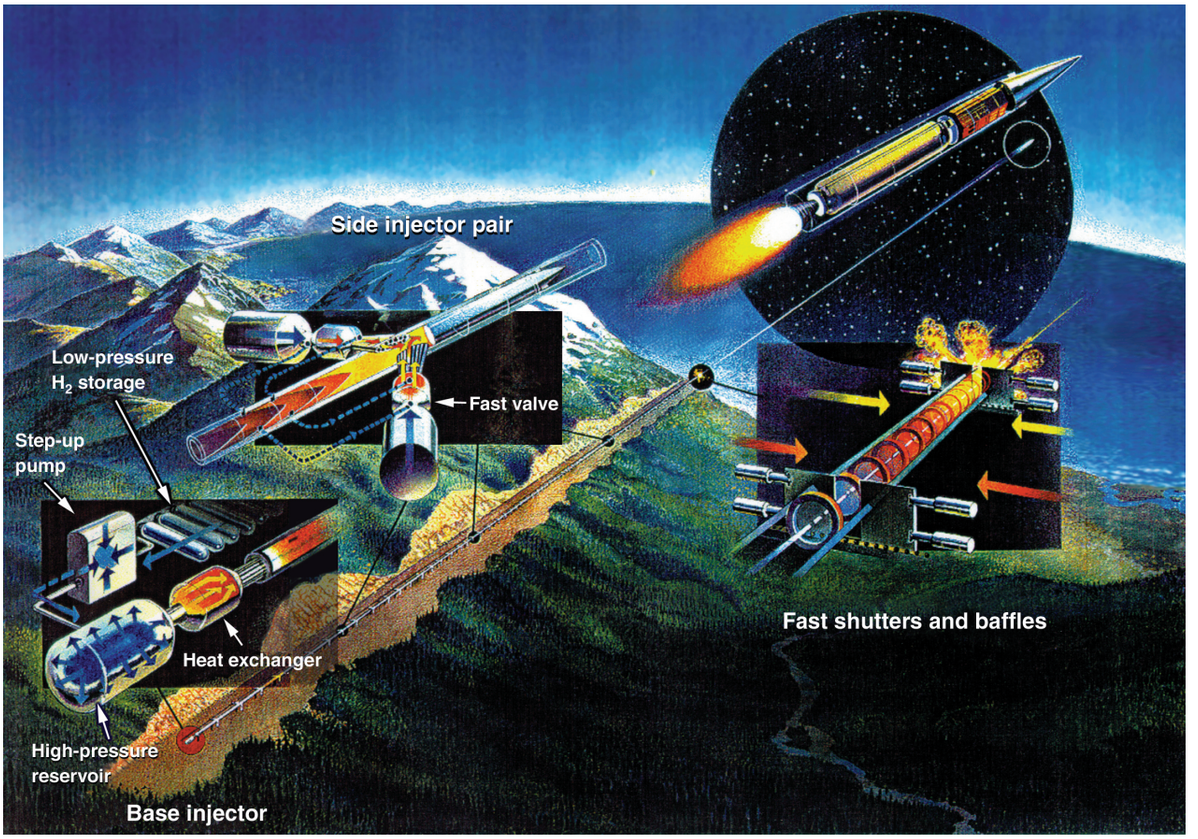

Figure 3. Launch system concept. A distributed-injection gun achieves high muzzle velocity with relatively low *g* loads by adding mass and energy along the barrel instead of just at the breech. The launch tube for the system under study is over 1.5 km long and uses 15 pairs of injectors to achieve a muzzle velocity of 7 km/s.

show that performance begins to decline if the working fluid is injected more than 10 launch tube diameters behind the projectile, and falls off rapidly after 50 launch tube diameters, requiring precision timing and valve opening times on the order of 1 ms near the muzzle.

The launcher will operate with approximately 10 million standard cubic feet of hydrogen. The hydrogen working fluid could be disposed of on every launch without appreciable environmental impact; however, its cost (≈$365K) is a significant fraction of the total launch cost. Thus, the hydrogen is captured with a series of baffles (a "silencer") and fast shutters at the muzzle, and returned through a scrubber system to the low-pressure storage reservoir for reuse. The pumping system is sized to complete hydrogen recovery in 2 h. Evacuation of the launch tube takes 1 h and is essential because the enclosed gas has a mass comparable to that of the launch package.

Figures 4 and 5 show results from a scaled simulation of the distributed-injection gas dynamics, using a base injector and two side injectors. The simulation is used to verify performance and aids in sizing system components. Both the launch mass and tube length (i.e., energy or number of injectors) have been scaled by 3/16, thereby preserving the 7-km/s muzzle velocity. The code employed here, SIDEHEAT, was developed by Hunter at Lawrence Livermore. It includes a real gas equation of state, working fluid wall friction, and heat

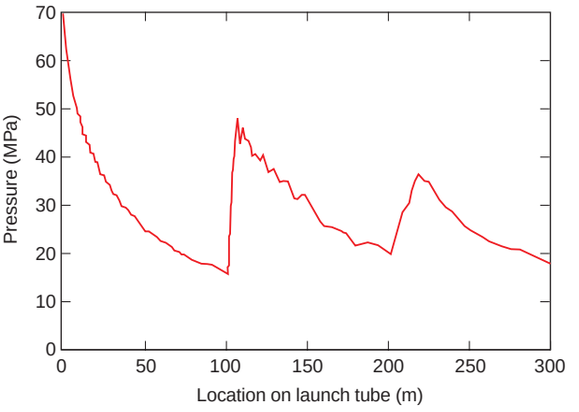

Figure 4. Simulated pressure at the base of the launch vehicle as a function of distance along the launch tube.

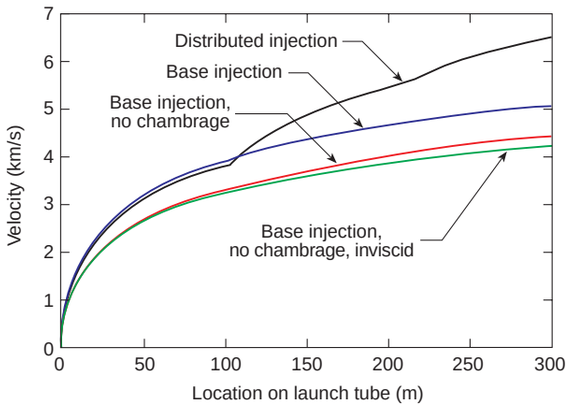

Figure 5. Vehicle velocity distribution along the launch tube. A launch tube has "chambrage" whenever the diameter of the high-pressure reservoir is greater than the launch tube diameter. Chambering the launcher improves performance.

loss to the walls, and simulates shocks with the Godonuv method.[9] Figure 4 shows details of the projectile base pressure, which are integrated in Fig. 5 to give velocity. Figure 5 also illustrates the sequential effects on velocity of viscosity, "chambrage," and distributed injection, assuming a fixed total reservoir volume and pressure. (A launch tube has chambrage whenever the diameter of the high-pressure reservoir is greater than the launch tube diameter.) In the simplest case, inviscid flow and no chambrage, the code reproduces the well-known analytic relation between the pressure and velocity ratios.[8]

Launch Vehicle

Figure 6 depicts the major components of the launch vehicle. The spacecraft is contained in a 0.17-m^3 compartment aft. The low drag configuration aeroshell (length/diameter ≈11) provides thermal protection and structural support, and is jettisoned after atmospheric egress. A single-stage solid-rocket motor fires prior to apogee and injects the spacecraft into a circular orbit. An integral attitude control system orients the projectile after the aeroshell is discarded, corrects for thrust misalignment during motor firing, and may be used for orbital trim.

The launch vehicle can be described as an "inverse" reentry vehicle, and employs similar methods for thermal protection. The aeroshell is constructed primarily of carbon composite and weighs 223 kg. Analytical[10] and computational[11] analyses of ablation predict approximately 7.6 cm of nose cone recession, although incorporation of an aerospike might reduce both drag and deformation during atmospheric egress. The power law body ($r = Ax^{0.65}$) with 7.5° base flare ensures both low drag (C_d = 0.016) and passive stability, although the margin of stability was estimated to be very small.[12]

As currently envisioned, the solid-rocket motor weighs 250 kg. It has a steel case (e.g., D6AC) and an NH_4ClO_4/Al propellant with a mass fraction of 0.84. The geometry allows for an expansion ratio greater than 20, giving a specific impulse (I_{sp}) of at least 270 s. With a 6080-N thrust and a burn time of 91 s, the motor supplies the required change in velocity (ΔV = 2.1 km/s) to orbit the spacecraft. About 14 kg are reserved for the hydrazine-fueled attitude control system. The system includes six thrusters (two pitch and four yaw/roll) with I_{sp} = 230 s. An additional 82 kg is allocated for the carbon composite sabot (not shown in Fig. 6) that supports and protects the launch vehicle while it is in bore.

A typical mission for a 700-km polar launch is illustrated in Fig. 7. At $t - 1$ h, the step-up pumps begin to charge the high-pressure reservoirs with hydrogen from the storage reservoir. As the countdown proceeds, the temperature is raised to operational level in the heat exchangers, and launch is initiated by switching the high-speed valve in the base injector. The position of the launch package is sensed in bore, and the side injector pairs are sequentially triggered. At t + 0.44 s, the launch vehicle exits the muzzle and sheds its sabot. The aeroshell is jettisoned at t + 300 s, when the launch vehicle is at an altitude of well over 500 km, and the attitude control system orients the launch vehicle for a motor firing at t + 545 s. After a 91-s burn, orbit is nominally achieved at t + 636 s. Figure 8 is a simulation of the launch vehicle's velocity profile during this mission.[13]

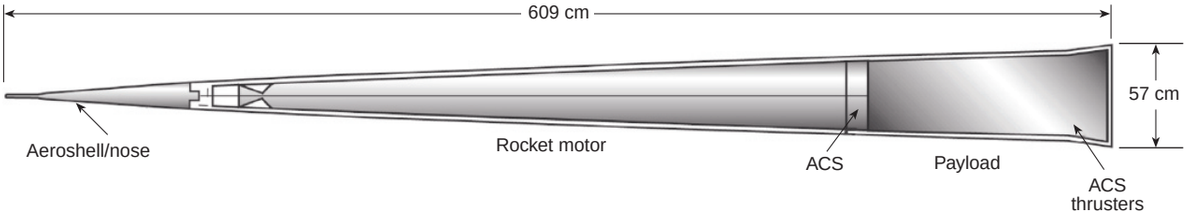

Figure 6. The ablation-cooled launch vehicle weighs 600 kg, including the 113-kg spacecraft it carries to orbit. The solid-rocket motor used for insertion is packaged with the aft end in front to move the center of gravity forward. The flare at the base of the vehicle moves the center of pressure rearward to achieve static stability (ACS = attitude control system).

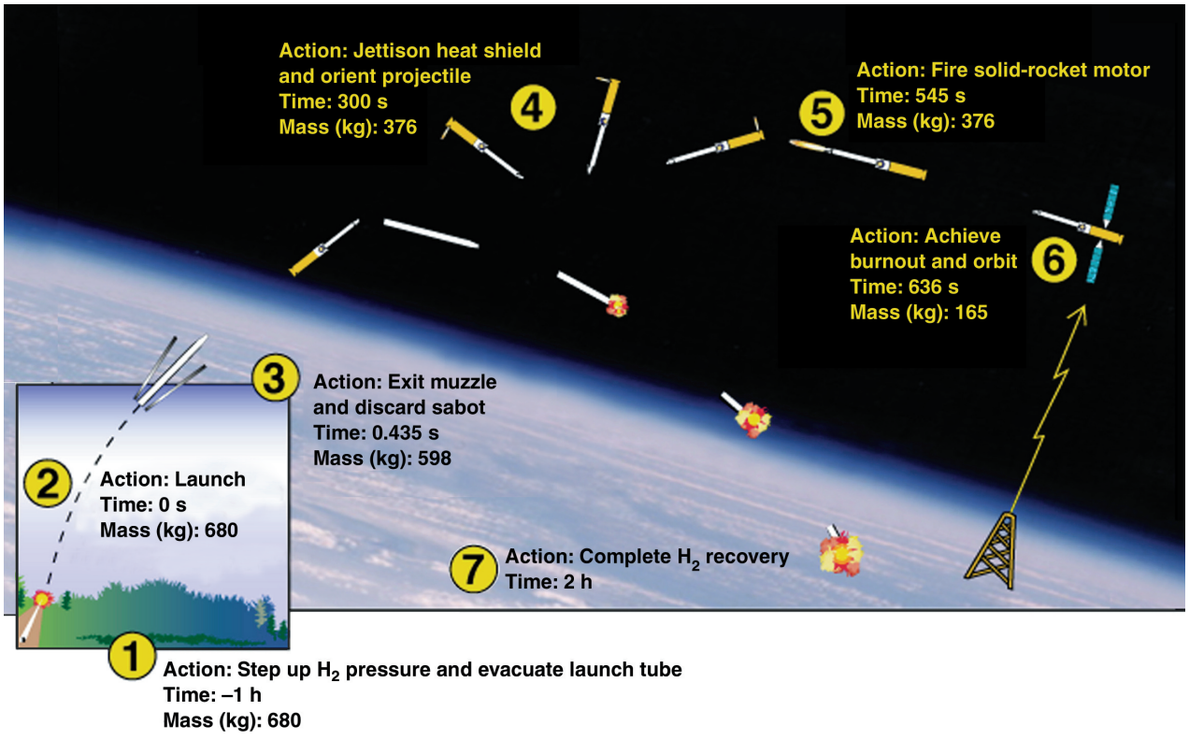

Figure 7. Launch sequence. The launch vehicle exits the gun in less than 0.5 s and crosses the outer edge of the atmosphere 20 s later. A 700-km orbit can be achieved in about 10.5 min. The entire sequence between launcher preparation and recovery takes about 3 h, so several launches per day may be possible.

Scaling and Performance Considerations

Practical considerations and the current state of the requisite technologies help to define the design and, given the unconventional nature of the gun launch concept, a conservative approach is prudent. For example, the conventional material used for launch tubes is steel, even though its melting point limits the working fluid temperature to less than 1700 K. The 1500 K working temperature assumed here further limits sound speed, and hence muzzle velocity, shifting more of the velocity burden to the injection motor. However, despite a conservative selection of material and operating margin, the overall system performance remains impressive.

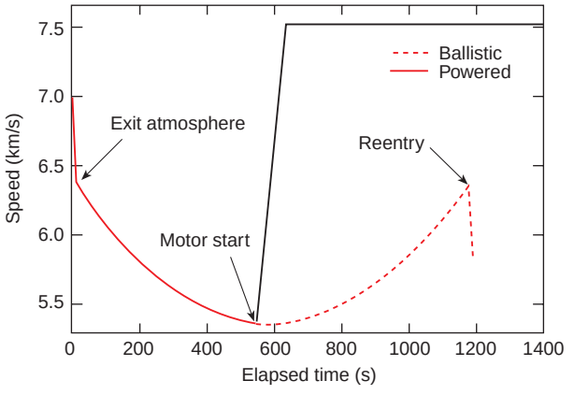

Figure 8. Variation of the speed of the launch vehicle from muzzle exit to orbit. If the solid-rocket motor fails to fire, the vehicle would follow a ballistic trajectory to reentry.

Many trade-offs can be made among launcher design, vehicle design, and the way the mission is executed. Examination of launch vehicle scaling reveals an important point and illustrates some of the trade-offs. The parameters such as muzzle velocity, orbital altitude, drag coefficient, and average base pressure are fixed. Under these conditions, the in-bore stresses are invariant because the system is scaled photographically, so the structural mass fraction can remain constant. However, a higher launch mass means a higher ballistic coefficient and therefore better penetration of the atmosphere. A shallower launch angle can then be tolerated, and is in fact necessary to reach a fixed apogee. The inherently higher angular momentum of the shallower trajectory reduces the ΔV requirement for the injection motor.

Of larger impact is the thermal protection scaling. Increasing the launch mass decreases the relative

amount of surface area requiring protection, but the higher ballistic coefficient and shallower launch angle yield a higher velocity and longer path length in the atmosphere. For the required range, surface area effects dominate aerothermal considerations, and relatively less shielding is required at higher launch mass. (These arguments do not hold indefinitely because, to a good approximation, the density profile in the atmosphere is exponential.) The net effect is that rocket motor and heat shield mass can be traded for spacecraft mass as the total launch mass increases. Figure 9 illustrates this behavior. Note that the spacecraft mass fraction exceeds that of conventional launch vehicles by an order of magnitude or more.

The launcher has been optimized for its mission, subject to certain assumptions about maximum desirable *g* loads, etc. However, the effect of off-optimum operation on performance must be determined, given that reorientation of a large launcher is difficult. Small inclination changes can be accomplished with the rocket motor but, as is well known, these changes significantly increase spacecraft mass. This fact is not necessarily true for launches to different altitudes. As Fig. 10 shows, altitudes below ballistic apogee can be reached with little change in the total required ΔV by entering a Hohmann transfer ellipse. Spacecraft mass will still likely increase to some extent to accommodate a more complex, two-pulse motor.

Technical Risks

A number of launcher technologies require testing and integration. The engineering of the injector is critical. Valves with throats having diameters of tens of centimeters must open within a few tens of bore diameters of the projectile's passing in a carefully timed sequence. That is, they must open precisely and repeatedly at "bullet"-type velocities. Preaccelerated valves for hydrogen capture, such as would be required at the muzzle, have been demonstrated (personal communication, D. Hayami, University of Alabama-Huntsville Aerophysics Laboratory, 19 Dec 1997), but reliability, maintainability, and synchronization remain issues for all of the high-speed valves. The principles of operation of the heat exchangers are understood, but further analysis and some experimentation are necessary to ensure proper throughput, function, and robustness in a regime that goes beyond previous experience. Finally, simulation of distributed-injection launcher performance is a valuable design tool, but code predictions must be validated against actual performance data. All of these requirements could be adequately tested with a heavily exercised, scaled prototype.

Several launch vehicle issues warrant further investigation. Thermal loads appear manageable using standard reentry vehicle materials and techniques, although the aerothermal environment for egress is more severe. Of particular concern is hypersonic stability, especially with respect to how it is affected by ablation. Analysis, simulation, and experimentation are essential.

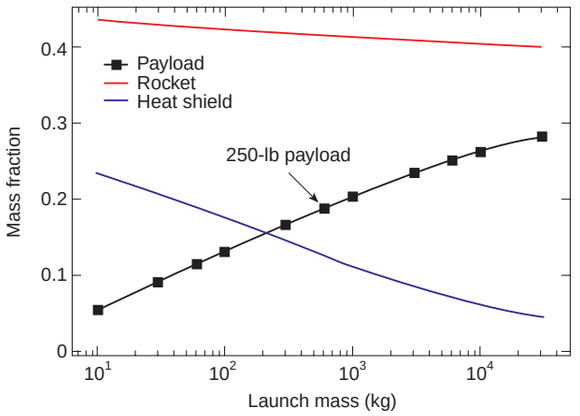

Figure 9. Launch mass scaling (sabot not included). The mass fraction devoted to thermal shielding decreases as the total launch mass increases because the relative amount of surface area requiring protection decreases. The rocket mass fraction also decreases owing to the increasing tangential velocity at apogee associated with shallower launch angles.

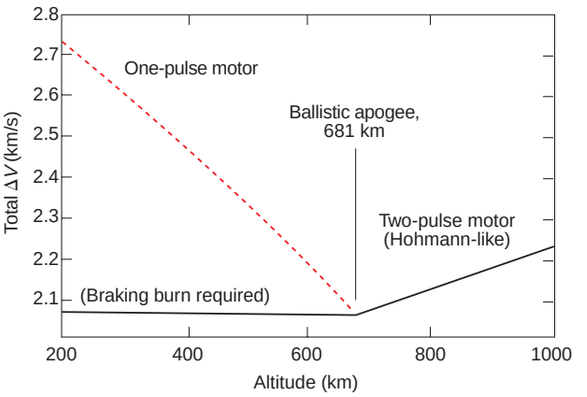

Figure 10. Adjustment of orbit altitude when the launch elevation is fixed. The difference in the velocity increase needed to reach a range of orbit altitudes is small, but a more complex two-pulse motor is required (V_m = 7 km/s, launch angle = 21°, β = 148,000 kg/m^2 [C_d = 0.016]).

SPACECRAFT SYSTEM

Subsystem Analysis

Traditionally, a spacecraft is designed to meet fixed launch vehicle parameters. In this study, however, we had the luxury of optimizing the gun, launch vehicle, and spacecraft to support a specific mission, and exploring departures from that mission as a result of launcher

constraints. This circumstance allowed an iterative loop between the launcher and spacecraft designs that normally is not available (Fig. 2).

The spacecraft was first defined using the set of system requirements given in Table 1. From that set, we derived the subsystem specifications shown in Table 2. We found that the subsystems most affected by the high-acceleration loads and other launcher limitations were the structural, power, and attitude determination and control (ADAC) subsystems. To handle the higher-than-normal launch loads, we assumed the spacecraft's primary support structure to be a simple ribbed cylinder. We examined four materials: titanium (Ti 6Al-4V), aluminum (Al 6061-T6 and Al 7075-T6), and a metal matrix composite (Al SiCp/6061-T6). We chose Al 7075-T6 as our primary structural material because of its relatively high strength, low cost, and good thermal conductivity. With the use of this alloy, the primary structure's mass fraction was 39%, which is considerably higher than the 8 to 15% fraction that is typical of spacecraft designed for conventional launchers.

We analyzed the power subsystem parametrically to determine how much power would be available from various solar array and battery configurations. Both silicon (Si) and gallium arsenide (GaAs) solar arrays were assessed in two body-fixed and two deployed configurations. The arrays were not designed to articulate, although articulation would probably be required in an operational system. The most powerful configuration was a deployable GaAs array that was about as long as the launch vehicle and had a lateral dimension defined by its mean inner circumference. The array could be stowed internally during transatmospheric flight, and would be capable of producing slightly more than 250 W.

We studied four types of batteries: nickel-hydrogen (NiH_2), lithium (Li) ion, sodium-sulfur (NaS), and nickel-cadmium (NiCd). We rejected NaS batteries because of their experimental nature and thermal requirements. Li-ion technology, while promising, was also rejected because of the battery's inability to meet the high number of discharge cycles associated with the mission's orbit. Although we would have preferred NiH_2 batteries, given their strong space legacy and high power density (approximately 1.6 times that of NiCd), they require about twice the packaging volume of NiCd batteries. The volume constraint makes them incompatible with the initial vehicle design. We also believe that, unlike NiCd batteries, they would be sensitive to high acceleration loads. If we chose NiCd batteries, the total power subsystem, including the solar array and associated electronics, would have a mass of approximately 30 kg, or about 26% of the total spacecraft mass. Together, the structure and batteries account for almost two-thirds of the total mass.

Items such as star cameras, reaction wheels, and spinning Earth horizon sensors were shown to have sensitivities to high acceleration loads, so some technology investments would be necessary to develop a survivable ADAC subsystem. We do not believe the design problems are insurmountable, however.

Table 3 shows the subsystem allocations of mass, volume, and associated mass fraction that were obtained after one design iteration. Assuming that the power system is sized adequately, we note that there is almost no mass available for the RF payload, implying that the mission cannot be carried out with the initial gun design. Given the limitations of time and funding, we were not able to converge on a spacecraft design that satisfied the original mission requirements. However, we obtained enough information during the analysis to uncover the major influences of high *g* loads and packaging constraints on subsystem design.

Table 2. Subsystem specifications.

Subsystem	Specification
Power	
Bus voltage	22–34 V
Average load	251 W
Battery	16.0 A·h
Attitude determination and control	
Roll	±0.6°
Pitch	±0.9°
Yaw	±1.2°
Propulsion (position maintenance)	
In track	±2.0 km
Cross track	±1.7 km
Orbit adjustment	
Fix inclination error	±0.057°
Fix apogee error	±14 km
Shift in orbit	±6°
TT&C	
Command uplink data rate	1 KB/s
Command downlink data rate	1 KB/s
Structures	
Quasi-static loads	2500 *g*

Note: TT&C = telemetry, tracking, and communication.

Generalized Results

The small mass fraction available for the RF payload does not imply that a complex telecommunications satellite cannot be launched with a gun, but rather that the initial sizing of the gun was too restrictive for the chosen mission. An RF payload places high demands

Table 3. Subsystem allocations after design iteration.

Subsystem	Weight (kg)	Volume (ft^3)	Mass fraction (%)
Attitude determination and control	10.6	0.34	9.3
Propulsion (wet)	18.3	0.72	16.1
Power	29.7	2.55	26.2
Structures	44.2	0.91	39.9
Thermal	3.1	0.10	2.7
Command and data handling	Part of payload		
GNS unit	1.3	0.10	1.1
TT&C	0.9	0.05	0.8
Harnessing	1.7	0.10	1.5
Available for payload	3.6	1.10	3.2
Total spacecraft mass	113.4	5.97	100

Note: TT&C = telemetry, tracking, and communication; GNS = GPS Navigation System.

on power and volume. In this section, we use the results of the subsystem analysis to generalize the results to other possible payloads. What payload power-mass combinations are compatible with a 113-kg spacecraft launched at 2500 *g*? In addressing this question, we allow for higher power density batteries and more advanced structural materials.

Figure 11a shows two sets of curves. The middle set is associated with a structural mass fraction of 39%, which corresponds to the use of an aluminum structure. The upper set assumes an advanced composite structure with a mass fraction of 20%. The separate curve at the bottom shows a "realistic" design, where the packaging density is limited to 450 kg/m^3 and (because of their volume efficiency and their legacy of high-acceleration applications) NiCd batteries are used. The curves in each set correspond to different battery technologies: NiCd, NiH_2, and "advanced technology," i.e., either Li-ion or NaS batteries.

Any point in the area underneath any of the curves in Fig. 11a is a possible design point within the class of spacecraft addressed in this study. For example, if one had a 20-kg payload that required 100 W, a 39% structural mass fraction would suffice, but an advanced technology battery would be required. If a 40-kg payload mass was required, then the structural mass fraction would have to drop.

Figure 11b shows the same set of curves for a spacecraft that does not require a propulsion system, but still must meet the other subsystem requirements, such as navigation and pointing. As the figure shows, when the propulsion system (18.3 kg) is removed from the spacecraft, a different set of curves is generated. Clearly, in this case, more power and mass are available to the payload without employing advanced technologies.

Major Technical Risks

Launch acceleration loads are 2 orders of magnitude higher than those encountered in conventional space launch. This is a large step for the space launch community, but the loads in question are survivable for many payload components using standard industry design practices. Many consumer electronic products can be made to survive >3000 *g* with a mass penalty of only a few percent. This result was demonstrated directly during the present work by subjecting cell phone handsets and other commercial electronics packages to high-acceleration loads in an air gun. Nevertheless, components such as the large optics in a star camera, reaction wheels, or spinning Earth horizon sensors will need special attention. Issues regarding packaging and deploying solar arrays and antennas are also very important.

Conventional packaging densities, coupled with the increased mass devoted to the support structure, can reduce the payload mass substantially. Gun-launched spacecraft will require considerably higher packaging densities than is the practice now, but with the industry looking toward micro- and nano-spacecraft, high-density designs may be possible in the future.

FINANCIAL ANALYSIS

Financial Model

The major premise shaping the financial analysis was that the gun-launched system would be a commercial entity, operating as a business that offers competitive returns to investors. Whereas our analysis does not fully address all of the issues inherent in the term "business operation," it provides significant insight and a solid foundation for future study.

The financial model provides a year-by-year representation of cash inflows and outflows for the launch complex based on selected physical and financial parameters. It has a 15-year planning horizon, with a time

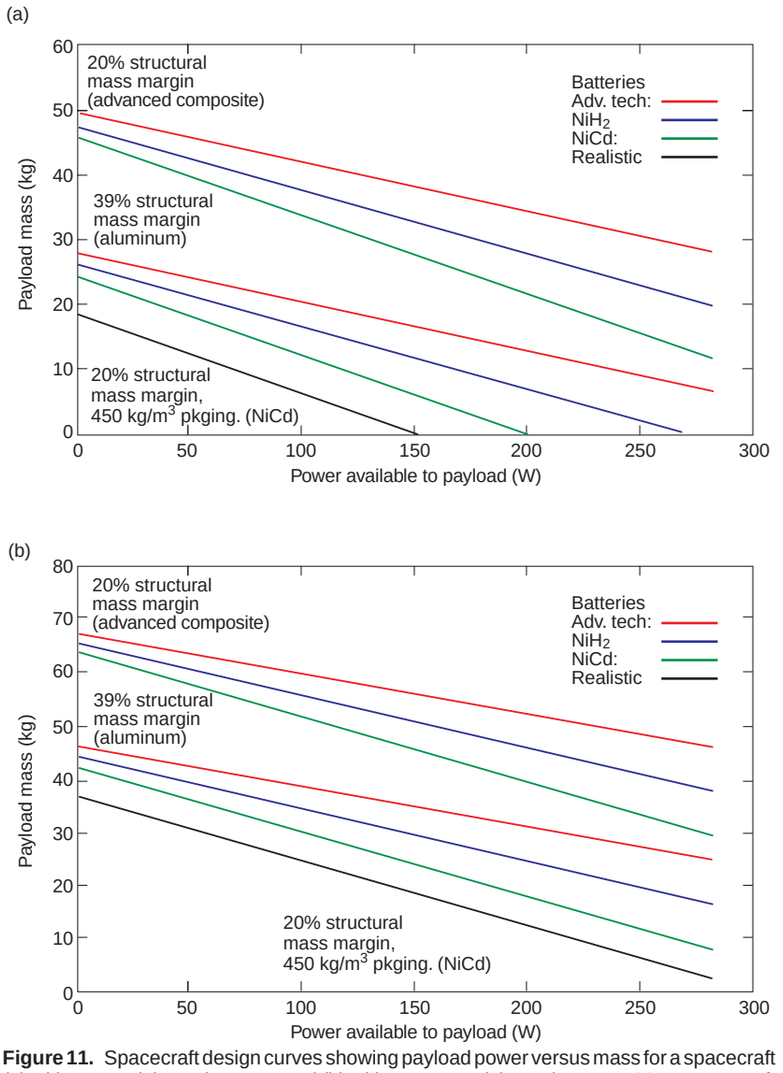

Figure 11. Spacecraft design curves showing payload power versus mass for a spacecraft (a) with a propulsion subsystem and (b) without a propulsion subsystem. Most spacecraft components are readily "*g* hardened" at 2500 *g*, but this results in higher mass fractions for the structure and power subsystems. The application of advanced materials and battery technologies can offset this increase in mass fractions. Any point beneath a selected "technology curve" in these plots represents a possible spacecraft payload. (Note: Energy densities = NiCd: 30 W·h/kg, NiH_2: 50 W·h/kg, Adv. tech: 140 W·h/kg).

resolution of 1 year. Several key assumptions were built into the model, and not subject to variation during the course of the analysis. We assumed that the first 3 years were devoted to the construction of the system. The maximum launch rate during the fourth year was taken to be either 50 per year or the prevailing yearly launch rate, whichever was less. This assumption allowed for possible construction delays and a "shakedown" period for launcher system operation. There was no allowance for "down time" for major maintenance or refurbishment. We also assumed that any major maintenance could be completed without affecting the yearly launch rate.

Construction Costs

Construction costs were broken down to a Level II Work Breakdown Structure (WBS). The WBS components included the launch tube, injectors, hydrogen storage, hydrogen heaters, valves, handling equipment, site work, etc. These costs were fully amortized by the end of the 15th year. We assumed that a quantity of funds was borrowed at the start of the program and that the funds not utilized for construction in a given year were invested at the prevailing interest rate (8% was used for all calculations). All funds borrowed for construction were expended by the end of the third year, according to a profile that assumed that 50% was expended in the first year, 25% in the second, and 25% in the third. The model automatically calculated the required funds based on the construction costs, the expenditure profile, and the interest rate. This calculation established the yearly construction loan payment. The actual cost figures were derived from estimates based on a mix of cost estimating relationships and analogous component estimates that were prepared for the construction of the JVL-200 (90-kg payload) launcher in Adak, Alaska.

Operating Costs

Operating costs were divided into fixed and variable costs. Fixed costs represented "housekeeping" costs that were independent of the number of launches per year. The fixed costs (payroll, supplies, and site maintenance) were taken to be $4 million per year, based on the JVL-200 launch cost estimates. Variable launch costs represented a "per-launch" cost including labor, hydrogen, etc., but did not include the cost of the launch vehicle. These variable launch costs were also based on the JVL-200 launch costs. The data provided variable costs for 75, 150, 300, and 600 launches per year. Variable costs were approximately $5200 per launch at a launch rate of 300 per year. We performed a log transformation on the data, and then based the costs on a linear regression model of the transformed data. This regression was used to

estimate the per-launch costs in the model for the varying launch rates under analysis.

The three cost elements of the launch vehicle were (1) the initial vehicle R&D costs, (2) the cost of the first vehicle (Y_1), and (3) the learning curve rate for launch vehicle production. The inclusion of these elements reflected the assumption that the business entity operating the launch complex would be responsible for developing and building the launch vehicle. The model also provided the option to use a fixed cost per vehicle so that the vehicles could be purchased from some other commercial source instead of being developed internally. These two approaches yielded slightly different results, due to the effects of the discount rate.

Cost Estimating Methods

We considered several methods for estimating the cost of the first launch vehicle. One method used a NASA model,[14] which provided a rough order-of-magnitude cost estimate for a missile having characteristics similar to the launch vehicle. More detailed estimates were based on subsystem-level pricing of the conceptual vehicle shown in Fig. 3, and on inflation-adjusted cost breakdowns for the Brilliant Pebbles[4] and HARP[2] vehicles. The latter estimating methods produced similar vehicle costs, ranging between $280,000 and $320,000 per vehicle. Costs associated with the launch vehicle were increasingly important in certain launch parameter scenarios, and so we chose to use the higher-fidelity approach in our work.

Several cost elements were not modeled because of the time that would have been required to analyze them. These elements included taxes, insurance, depreciation, range clearance costs, and the cost of a major refurbishment of the launch complex. No land acquisition costs were allocated. We assumed that any environmental impact approvals would be obtained with reasonable processing costs that were included in the construction costs. We further assumed that there would be no additional costs or delays to the project due to litigation, strikes, or other causes. Representative values for several key financial parameters are contained in Table 4.

Table 4. Financial parameters (representative values).

Parameter	Value
Interest rate (per year)	8%
Amortization period (years)	15
Spacecraft weight (kg)	113
Price per kg	$3,486
Initial launch vehicle cost	$320,000
Launch vehicle learning curve rate	90%
Average launch vehicle cost	$109,589
Launcher construction costs	$298,000,000
Yearly construction loan amortization	$32,928,784
Fixed launcher operating costs	$4,000,000
Variable launcher operating costs	$15,551,000
Average yearly launch vehicle costs	$32,876,584
Launches per year	300
Yearly gross revenue	$118,597,576
Internal rate of return	8%
Net present value	$0

Cost Analysis

We can illustrate the basic results of the analysis with a few of the graphs and tables we developed in the course of the cost analysis. All the graphs presented in this section will be for the values indicated in Table 4 unless otherwise indicated.

An example of an income stream graph is shown in Fig. 12, corresponding to an internal rate of return (IRR) of 20% (see the boxed insert). In this case, the operation turns its first yearly profit in year 5, but cumulative cash flow is not positive until year 9. Analyses of this type provided temporal income data that allowed us to predict yearly revenue and profit margins as model parameters were varied.

We also analyzed the major cost drivers for the operation of the launch system, given reasonable estimates of most of the costs involved in calculating the total ownership cost. Table 5 illustrates two typical potential operating scenarios and highlights a key result: reductions in launch vehicle cost offer the greatest opportunity for driving the launch costs down further.

Initially we thought that the launcher would probably be most cost-effective in a "mass market," with a launch rate measured in hundreds of launches per year. But when we varied the launch rate and looked at the required revenue stream expressed in terms of dollars per launch rather than dollars per kilogram, we found possible ways of operating the system profitably (see

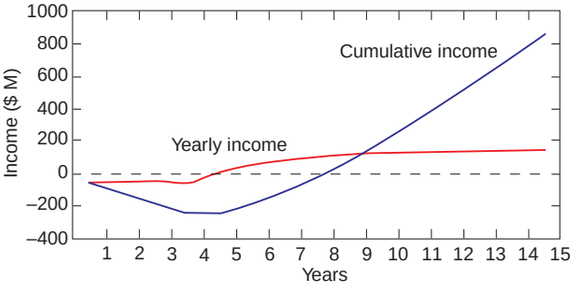

Figure 12. Yearly and cumulative income as a function of time. In this example, the internal rate of return is 20%.

AFFORDABILITY METRICS AND CONCEPTS

We used several standard financial metrics as our figure of merit (FOM) for affordability. This insert provides a quick review of those measures and concepts discussed in the article. A more complete review of IRR and NPV can be found in Blanchard and Fabrycky.[15] Stewart et al.[16] contains an excellent discussion of learning curves.

NPV is a metric that quantifies the value of an income stream (which can contain either positive or negative cash flows in each period) over a period of time, taking the interest rate into account. In mathematical terms:

$$\mathrm{NPV} = \sum_{t=0}^{n} F_t (1+i)^{-t}, \qquad (1)$$

where

NPV = net present value,
t = time period in years,
n = number of years, and
F_t = net cash flow in year t.

The IRR is a measure of profitability. It is the interest rate that, when applied to a stream of cash flows, causes the NPV to be 0. It is analogous to the return on a mutual fund or certificate of deposit. Mathematically, IRR is defined as the interest rate i^* such that

$$0 = \sum_{t=0}^{n} F_t (1+i^*)^{-t}. \qquad (2)$$

All other terms are as defined previously for NPV. NPV and IRR were both used as parameters and as FOMs in the analysis.

The learning curve, or progress function, is a means of quantifying how familiarity and experience with the completion of a product lead to greater efficiency and cost reduction in production. Learning curves are frequently expressed as percentages. An 85% learning curve implies that a cost reduction of 15% occurs when the number of articles is doubled. The fourth unit produced would cost 85% of the cost of the second unit, the eighth unit would cost 85% of the fourth unit, and so forth. Mathematically, the learning curve relationship is defined by the following equation:

$$Y_t = Y_1 t^b, \qquad (3)$$

where

t = unit number, and
Y_t = cost of unit number t.

The exponent b is defined by

$$b = \frac{\ln(m)}{\ln(2)},$$

where m is the learning curve rate expressed as a decimal. The learning curve rate and initial unit cost of the launch vehicle were used as parameters in the analysis.

Table 5. Cost element breakdown.

	Percent of total cost	
Cost area	300 launches/year	52 launches/year
Construction	9	30
Fixed operating	1	4
Variable operating	4	4
Launch vehicle	86	62

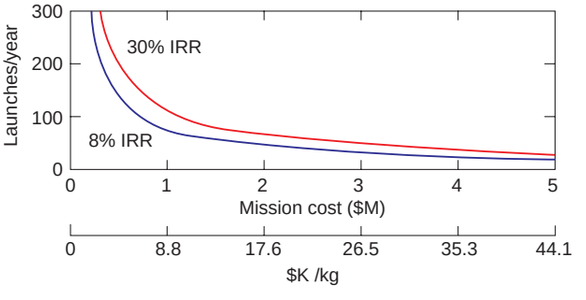

Figure 13. Launch costs. When private development, a reasonable interest rate (8%), and a 15-year amortization schedule are assumed, the total mission cost of a gun-based satellite launch service looks promising. An internal rate of return (IRR) of 8% represents "break-even" operation. When the IRR is 30%, investors might be interested.

Fig. 13). The lower trace on Fig. 13 shows those combinations of total mission cost and launch rate that result in a break-even situation (net present value [NPV] = 0; see the boxed insert). The upper trace shows those combinations that resulted in an IRR of 30%. (This value was chosen as representative of the minimum IRR needed to make the launch system attractive compared to alternative technology investments.) Analysis of graphs such as these led us to consider launch rates on the order of one per week. Although the cost per kilogram in this regime is much higher, the cost of approximately $2.5 million per launch is within the typical budget of small satellite researchers.

A few comparisons with conventional launch systems help put these results in perspective. Boeing's new Delta 3 launcher (now being tested in the United States) will be able to place a 6100-kg payload into a 700-km Sun-synchronous (98°) orbit at a cost of about

$12,300/kg.[17] The large European rocket, Ariane 5 (also under test), is designed to launch 10,000 kg to the same orbit for $15,000/kg. For the purposes of comparison, assume that a spacecraft in the 100-kg class could ride on these systems as a secondary payload at the same specific cost (dollars/kilogram). Assume further that to be sufficiently attractive, the gun system would have to undercut conventional prices by, for example, a factor of 2. With these assumptions, we see from Fig. 13 that hundreds of launches per year would be needed to make the venture competitive, if specific costs were the only consideration.

A more direct comparison can be made to the Pegasus launch system, which was designed specifically to launch small satellites. Pegasus XL can place a 250-kg payload into a 700-km Sun-synchronous orbit at a total cost of $14 million ($56,000/kg). The gun system fares well in this arena, showing an advantage of about a factor of 3 in total mission cost.

However, these comparisons oversimplify the problem of financial assessment. Differences in launch rate capacity, launcher availability, schedule reliability, infrastructure subsidization, and specific mission requirements are among the myriad factors that can affect the final judgement.

OVERALL ASSESSMENT

We conclude that placing small satellites into orbit using a distributed-injection, light-gas gun is technically feasible, provided that certain critical developments are made. For the launcher, the key components are fast-acting, high-flow-rate valves and a durable, high-temperature, high-pressure hydrogen heater. Thermal protection, aerodynamic stability, and packaging efficiency are significant problems for the launch vehicle.

Because of the large power levels required for high-throughput global telecommunications, our initial design iteration indicated that 100-kg spacecraft cannot meet the requirements of the reference mission, given the limits on payload mass and volume. In broadening the mission set, however, we found that a large range of useful, less power-intensive payloads and missions was possible. The actual range of achievable payload weight and power depends on the level of technology incorporated in the spacecraft structure and batteries, as well as the required level of on-orbit propulsion.

Our economic analysis showed that a payload-to-orbit cost of approximately $5500/kg would be required to yield an IRR of 30%, if the launch rate could be pushed to 300 per year. At the same specific launch cost, the operation would break even with 150 launches per year. Whereas this cost is within the bounds of present rates, the cost of conventional launches is likely to decrease in the future as new and upgraded launch vehicles enter the competition. As a result, we have some concern about the market attractiveness of the light-gas gun launcher for applications in which specific launch cost is important. Complexities are likely to arise when designing a system for a gun environment, and even 150 launches per year go beyond current projections for small satellites.

However, the gun launch system looks very favorable when total mission costs are considered. With a launch rate as low as one per week, a total mission cost of approximately $2.5 million would yield an IRR of 30%, and a total mission cost as low as $1.5 million would permit break-even operation. These mission costs are considerably less than current systems and provide for some interesting possibilities for small satellite operations.

CURRENT WORK

Whereas the telecommunications mission was useful for uncovering technical issues, other missions are more suited to gun launching. In particular, in the second phase of our work, we are looking at the use of gun-launched spacecraft to service or resupply constellations of satellites on orbit. This application can make use of the relatively inexpensive, on-demand operation inherent in gun-launched systems. The short duration (days to several weeks) and low power requirements associated with the mission eliminate the need for large deployable structures, which might otherwise pose difficulties for a high-density design. Our preliminary analysis indicates that such a mission is technically possible and might be cost-effective. We are presently defining a gun-launched spacecraft for this purpose and developing a concept of operations for its use.

Because the majority of serviceable components and supplies have a high tolerance to *g* loads, we are also reconsidering the basic designs of the gun and launch vehicle. Operating at higher *g* loads might lead to a shorter, less-expensive (and perhaps trainable) launcher. Reducing the muzzle velocity would also shorten the gun and diminish the thermal protection problem, at the expense of requiring a more complicated multistage launch vehicle.

When the spacecraft mass, volume, and maximum *g* loads are defined, and optimal conceptual designs for the launcher and vehicle are developed, we will analyze the cost and general performance of the system. Whether DARPA's interest in gun launchers will continue depends on how well the concept compares to alternative approaches.

REFERENCES

[1]Gilreath, H. E., Driesman, A. S., Kroshl, W. M., White, M. E., Cartland, H. E., et al., "The Feasibility of Launching Small Satellites Using a Light-Gas Gun," in *Proc. 12th AIAA/USU Conf. on Small Satellites*, Paper No. SSC98-III-6 (Aug 1998).

[2]Murphy, C. H., and Bull, G. V., "Gun-Launched Sounding Rockets and Projectiles," *Ann. NY Acad. Sci.* **140**, 337 (1966).

[3]Bull, G. V., Lyster, D., and Parkinson, G. V., *Orbital and High-Altitude Probing Potential of Gun-Launched Rockets*, Report R-SRI-H-R-13, Space Research Institute, McGill University, Montreal, Canada (Oct 1966).

[4]"Earth-to-Orbit Hypervelocity Launchers for Deploying the Brilliant Pebbles System," in *Vol. IV: Hypervelocity Light Gas Gun Report*, LLNL Report AD-B150944, Livermore, CA (Nov 1990).

[5]Gilreath, H. E., Fristrom, R. M., and Molder, S. "The Distributed Injection Ballistic Launcher," *Johns Hopkins APL Tech. Dig.* **9**(3), 299 (1988).

[6]Higgins, A. J., "A Comparison of Distributed Injection Hypervelocity Accelerators," in *Proc. 33rd AIAA/ASME/SAE/ASEE Joint Propulsion Conf. & Exhibit*, AIAA 97-2897, Seattle, WA (Jul 1997).

[7]Tidman, D. A., and Massey, D. W., "Electrothermal Light Gas Gun," *IEEE Trans. Mag.* **29**, 621 (1993).

[8]Siegle, A. E., "Interior Ballistics of Guns," *Prog. Astronaut. Aeronaut.* **66** (1979).

[9]Peyret, R., and Taylor, T. D., *Computational Methods for Fluid Flow*, Springer-Verlag, New York, p. 112 (1982).

[10]Tauber, M. E., *A Review of High-Speed, Convective, Heat-Transfer Computation Methods*, NASA Technical Paper 2914 (1989).

[11]*ABRES Shape Change Code (ASCC86)*, Acurex Corp., Aerotherm Div. for Headquarters Ballistic Missile Office/MYES (Mountain View, CA), Contract Number F04704-83 C-0024 (1986).

[12]Parthasarathy, K. N., *Light Gas Gun Assessment Study: Aerodynamic Analysis*, A1D-3-98U-046, JHU/APL, Laurel, MD (16 Jul 1998).

[13]*Calculation of Missile Earth Trajectories (COMET)*, RAND-R-3240-DARPA/RC Rand Corp., Santa Monica, CA (1989).

[14]*Advanced Missions Cost Model*, NASA, available at http://www.jsc.nasa.gov/bu2/AMCM.html (accessed 28 Jan 1999).

[15]Blanchard, B. S., and Fabrycky, W. J., *System Engineering and Analysis*, Prentice Hall, New Jersey (1990).

[16]Stewart, R. S., Wyskida, R. M., and Johannes, J. D., *Cost Estimator's Reference Manual*, 2nd Ed., Wiley Interscience, New York (1995).

[17]"Launchers of the World," *Int. Space Industry Report* **2**(13), 22–23 (3 Aug 1998).

ACKNOWLEDGMENT: This work was supported by the Tactical Technology Office of DARPA under Contract MDA972-96-D-0002, DARPA Order #0025, Task VRB. The DARPA Program Manager for this effort is Lt. Col. Walter Price.

THE AUTHORS

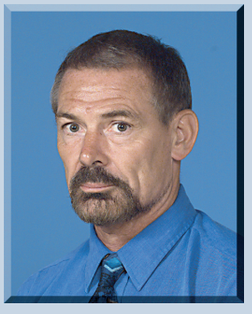

HAROLD E. GILREATH is a Principal Staff Engineer in the Milton S. Eisenhower Research and Technology Development Center (RTDC) at APL. He received his B.S. (1964), M.S. (1966), and Ph.D. (1968) degrees in aerospace engineering from the University of Maryland, where he also taught courses in aerodynamics and propulsion. He joined APL in 1968 as a member of the Hypersonic Propulsion Group and conducted theoretical and experimental research on advanced missile propulsion systems. Dr. Gilreath became a member of APL's Submarine Technology Department at its inception in 1978 and was appointed Chief Scientist of the Department in 1980. He joined the Milton S. Eisenhower Research Center (now the RTDC) in 1985. Since then, he has conducted research on many topics such as high-speed and stratified flows, groundwater mechanics, interior ballistics, and drag reduction. His e-mail address is harold.gilreath@jhuapl.edu.

ANDREW S. DRIESMAN is a member of APL's Senior Professional Staff. He received his B.S. in electrical engineering and geology from Tufts University in 1985. Prior to joining APL in 1997, he spent 12 years working for the Air Force Research Laboratory (AFRL) in Bedford, Massachusetts. At AFRL, he provided systems engineering support to the Clementine 2 mission, as well as several Ballistic Missile Defense Organization efforts. He is currently the Spacecraft Systems Engineer for NASA's STEREO mission. His e-mail address is andrew.driesman@jhuapl.edu.

WILLIAM M. KROSHL earned a B.A. in economics from Northwestern University in 1975 and an M.S. in operations research from the Naval Postgraduate School in 1988. He joined APL's Joint Warfare Analysis Department in 1997. He has been working on a variety of operations research projects, concentrating on affordability and risk analysis. Before joining APL, he served 21 years of active duty in the Navy and retired with the rank of Commander. While on active duty, Mr. Kroshl served on the faculty of both the Operations Research Department of the Naval Postgraduate School, Monterey, California, and the Mathematics Department, U.S. Naval Academy, Annapolis, Maryland. He spent over 12 years on sea duty on five different Navy surface ships. His e-mail address is william.kroshl@jhuapl.edu.

MICHAEL E. WHITE earned B.S. and M.S. degrees in aerospace engineering from the University of Maryland. He has an extensive background in aerospace engineering with particular emphasis on high-speed aerodynamics and propulsion. His experience includes the application of computational tools to the design and analysis of high-speed vehicles and the experimental assessment of hypersonic air-breathing propulsion systems. In addition, he has considerable experience in program and line management gained through his roles as Program Manager for the National Aerospace Plane (NASP) Program and Assistant Supervisor of the Propulsion Group, respectively. Mr. White came to APL in 1981 and was appointed to the Principal Professional Staff in 1991. He is currently the Program Area Manager for Advanced Vehicle Technologies in the Milton S. Eisenhower Research and Technology Development Center. His e-mail address is michael.white@jhuapl.edu.

HARRY E. CARTLAND earned an A.B. degree in chemistry from Cornell University in 1980. He received his Ph.D. in physical chemistry in 1985 from the University of California at Berkeley. He then spent 7 years on active duty in the U.S. Army, where he served in a number of assignments including as a faculty member at the U.S. Military Academy and as a research officer at the Ballistic Research Laboratory. Dr. Cartland left the Army in 1992 and spent 6 months as a visiting scholar at Duke University before assuming his present position. He is currently Physicist and Special Project Leader in the Engineering Department at Lawrence Livermore National Laboratory. His e-mail address is cartland1@llnl.gov.

JOHN W. HUNTER received his undergraduate degree from the University of California at San Diego and a Ph.D. in particle physics from the College of William and Mary. From there he joined the staff of the Lawrence Livermore National Laboratory, and started the Super High Altitude Research Project (SHARP). SHARP was designed as a technology demonstrator for gun launch to space and, at the time, was the world's largest light-gas launcher. Dr. Hunter currently runs JH&A, a private consulting business based in San Diego. His e-mail address is shelleen@pacbell.net.